General Disclaimer

One or more of the Following Statements may affect this Document

- This document has been reproduced from the best copy furnished by the organizational source. It is being released in the interest of making available as much information as possible.

- This document may contain data, which exceeds the sheet parameters. It was furnished in this condition by the organizational source and is the best copy available.

- This document may contain tone-on-tone or color graphs, charts and/or pictures, which have been reproduced in black and white.

- This document is paginated as submitted by the original source.

- Portions of this document are not fully legible due to the historical nature of some of the material. However, it is the best reproduction available from the original submission.

9950-864

CDRL No. 181
DRD No. QT

JPL Contract No. 956381
QR-10085-02

EVALUATION OF THE ION IMPLANTATION PROCESS FOR PRODUCTION OF SOLAR CELLS FROM SILICON SHEET MATERIALS

Quarterly Technical Report No. 2

JET PROPULSION LABORATORY
CALIFORNIA INSTITUTE OF TECHNOLOGY
PASADENA, CA 91103

spire

CDRL No. 181
DRD No. QT

QR-10085-02
June 1983

EVALUATION OF THE ION IMPLANTATION PROCESS FOR PRODUCTION OF SOLAR CELLS FROM SILICON SHEET MATERIALS

Quarterly Report No. 2
For Period Covering: 1 April - 1 July 1983

Contract No. 956381

Jet Propulsion Laboratory
4800 Oak Grove Drive
Pasadena, CA. 91009

Prepared by: Mark B. Spitzer
Principal Investigator

Approved by: Robert G. Wolfson
Program Manager

SPIRE CORPORATION
Patriots Park
Bedford, MA 01730
(617)-275-6000

TABLE OF CONTENTS

LIST OF ILLUSTRATIONS

LIST OF TABLES

1.0 OBJECTIVES

The objective of this program is the investigation and evaluation of the capabilities of the ion implantation process for the production of photovoltaic cells from a variety of present-day, state-of-the-art, low-cost silicon sheet materials. Task 1 of the program concerns application of ion implantation and furnace annealing to fabrication of cells made from dendritic web silicon. Task 2 comprises the application of ion implantation and pulsed electron beam annealing (PEBA) to cells made from SEMIX, SILSO, heat-exchanger-method (HEM), edge-defined film-fed growth (EFG) and Czochralski (CZ) silicon.

The goals of Task 1 comprise an investigation of implantation and anneal processes applied to dendritic web. A further goal is the evaluation of surface passivation and back surface reflector formation. In this way, processes yielding the very highest efficiency can be evaluated.

Task 2 seeks to evaluate the use of PEBA for various sheet materials. A comparison of PEBA to thermal annealing will be made for a variety of ion implantation processes.

2.0 MATERIALS

Various sheet materials were procured for use in the program. These materials are summarized in Table 1. For some of the materials, there is a large variation in resistivity, as indicated. In addition, the thickness of the wafers is quite variable. During the second quarter, new SEMIX slices were received (Lot 2). These slices were etched in 6-1-1 to remove saw damage.

3.0 WORK PERFORMED

Work in this quarter has focused on the study of furnace anneal parameters for various sheet materials. Two groups of materials were processed; the first consisted of EFG, SILSO, HEM and CZ, and the second consisted of SEMIX and CZ. The materials were separated in this way because the SEMIX was not available at the start of the quarter when the matrix was started. Consequently, data on the SEMIX group is not available at this time.

TABLE 1.
CHARACTERISTICS OF SHEET MATERIALS PROCURED
FOR USE IN THE PROGRAM

Growth	Source	Resistivity	Surfaces	Comments
1. Dendritic Web				
Lot 1	Westinghouse	2-10 ohm-cm	As Grown	Std. Material Dendrites Removed
Lot 2	Westinghouse		As Grown	Low Stress
2. SEMIX				
Lot 1	JPL/ASEC	2 ohm-cm	ETCHED	Thin (~150 μm)
Lot 2	SEMIX	2 ohm-cm	As Grown	
3. EFG				
Lot 1	JPL/ASEC	2 ohm-cm	As Grown	
Lot 2	Mobil Solar		As Grown	
4. SILSO				
Lot 1	Wacker	5-10 ohm-cm	ETCHED	
5. HEM				
Lot 1	JPL/ASEC	6 ohm-cm	ETCHED	
Lot 2	Crystal Systems		ETCHED	
6. Single Crystal				
Lot 1	Wacker	10 ohm-cm	POL	100 CZ
Lot 2	Wacker	1 ohm-cm	POL	111 FZ

Table 2 lists the process steps used for device fabrication. Various anneals were studied and each consisted of a ramp from 550°C to an activation step, 15 minutes at the activation temperature, ramp back to 550°C, followed by 550°C for one hour, all in following dry N_2. Cells were fabricated from all materials with the following activation temperatures: 850°C, 750°C, 650°C and 550°C. No AR coatings were applied. The cells to be reported on in the next section were all co-processed.

TABLE 2

SHEET MATERIAL n^+p CELL PROCESS SEQUENCE

1.	CLEAN	
2.	IMPLANT FRONT	
	Ion Species	$31p^+$
	Ion Energy	5 kev
	Dose	2.5×10^{15} ions/cm^2
3.	ANNEAL	
4.	EVAPORATE BACK METALLIZATION	
	Al-Ti-Pd-Ag	
5.	SINTER	
6.	PHOTOPATTERN FRONT	
7.	EVAPORATE FRONT METALLIZATION	
	Ti-Pd-Ag	
8.	METAL LIFTOFF	
9.	SINTER	
10.	PLATE FRONTS	
	10 μm of Ag	
11.	SAW TO 2cm x 2 cm	
12.	TEST	

4.0 SUMMARY OF DATA

All cells were tested under simulated AM1 conditions (100 mW/cm^2). Temperature was maintained at 28°C by a water-cooled test block. None of the cells have AR coatings. The CZ group was the control group for this experiment. Other materials studied were EFG, SILSO and HEM. The CZ performance achieved was typical of that obtained with 10 ohm-cm wafers processed without a back surface field (BSF). In this experiment, all cells have evaporated Al-Ti-Pd-Ag contacts; the Al was sintered at 400°C (not alloyed, which would have formed a BSF). It is important to note that the sample size for the data to be reported is small; only a few cells were fabricated for each matrix element. In analyzing the trends indicated by the data, variations must be compared to naturally-occuring variation in the material itself.

4.1 CZ Control Group

Table 3 lists the cell performance for the control group. The cells are compared to the 3-step baseline anneal reported in Quarterly Report No. 1. Note that in this work, better results were obtained with a simpler anneal. This indicates that either the 5 keV $^{31}P^+$ implant utilized in the present experiment is superior to the 10 keV $^{31}P^+$ implant utilized in the baseline study, or perhaps that the diffusion length was degraded by the baseline process. The FF is also better than that obtained in the baseline process indicating that the cell improvement may be the result of improved processing techniques.

Examination of the data in Table 3 indicates that higher temperatures are preferred for processing of CZ using a two-step anneal. The higher temperatures yield better activation of the dopant thus reducing sheet resistance losses, as indicated by the dark I(V) curves shown in Figure 1.

The external quantum efficiency of the control wafers has been measured and is shown in Figure 2. Increasing the activation temperature causes a decrease in the blue response. This is attributed to an increase in junction depth owing to diffusion during the anneal. The anomalous drop in red response for the 750°C sample is probably the result of decreased diffusion length. Other materials co-processed with the CZ wafer do not show degraded red response indicating that the anomaly is probably confined to the control wafer. Nevertheless, this data point must be considered when analyzing data for the other materials.

TABLE 3. AM1 PERFORMANCE OF THE CZ CONTROL GROUP.

Activation Temperature	Voc (mV)	Jsc (mA/cm^2)	FF (%)	Eff (%)	Eff x 1.45 (%)
550°C	526 (001)	24.3 (0.1)	71.1 (0.8)	9.09 (0.1)	13.2 (0.1)
650°C	529 (001)	24.3 (0.04)	71.9 (1.1)	9.24 (0.14)	13.4 (0.2)
750°C	533 (001)	23.9 (0.1)	75.2 (0.3)	9.60 (0.05)	13.9 (0.1)
850°C	543 (003)	23.9 (0.1)	77.1 (0.6)	10.0 (0.1)	14.5 (0.1)
3-Step*	533 (002)	22.3 (1.8)	73.5 (3.0)	9.07 (0.43)	13.2 (0.6)

NOTES: Insolation level is 100 mW/cm^2. T = 28°C. Area = 4 cm^2. Standard deviation shown in parenthesis. The 3-step anneal data are reproduced from the baseline experiments.

It is important to note that these cells have no AR coating or BSF. AR coatings would raise the J_{sc} by 45%; BSFs would raise V_{oc} by 10%. Efficiency with such features would be greater than 15%.

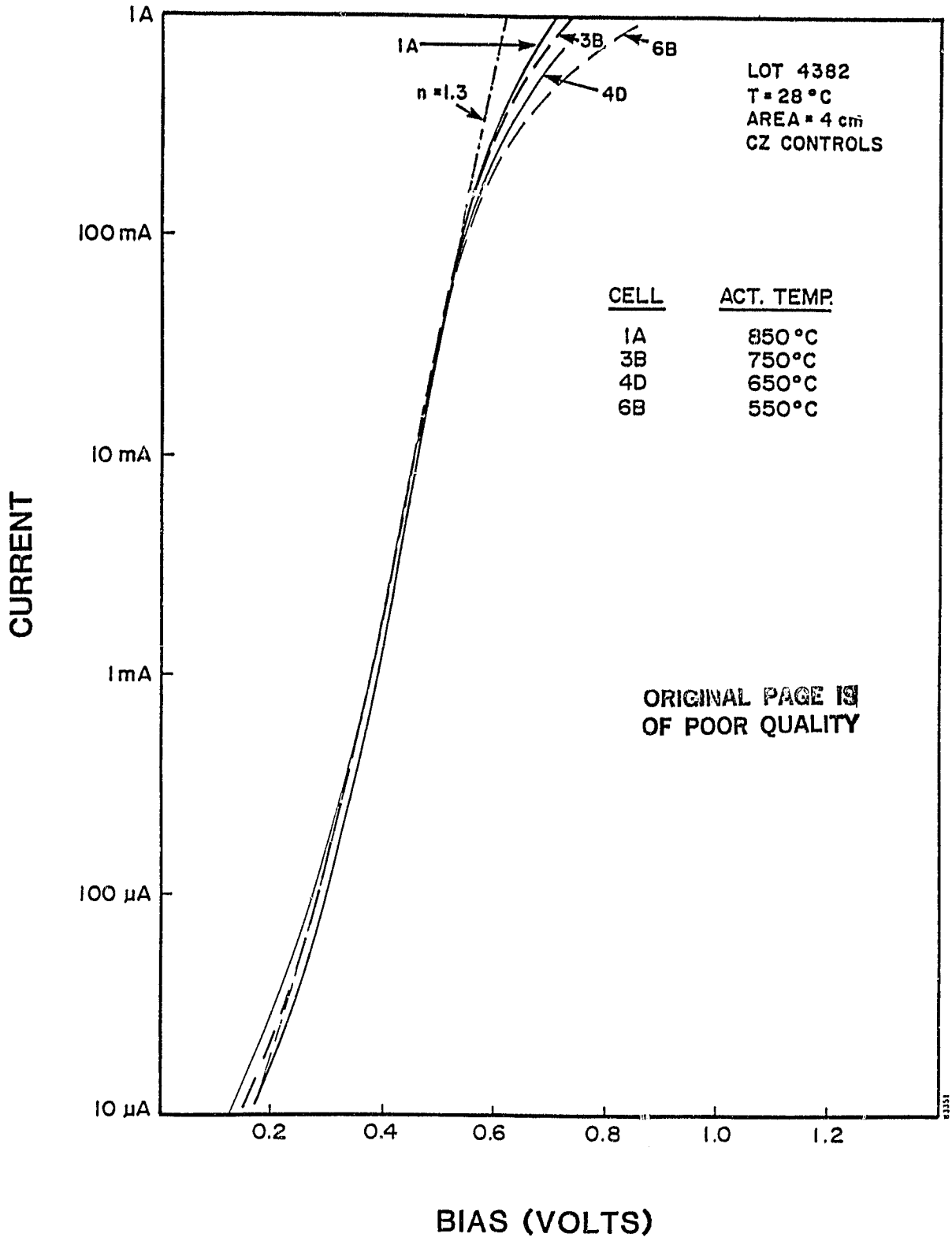

FIGURE 1. DARK I-V CHARACTERISTICS OF THE CZ CONTROL CELLS

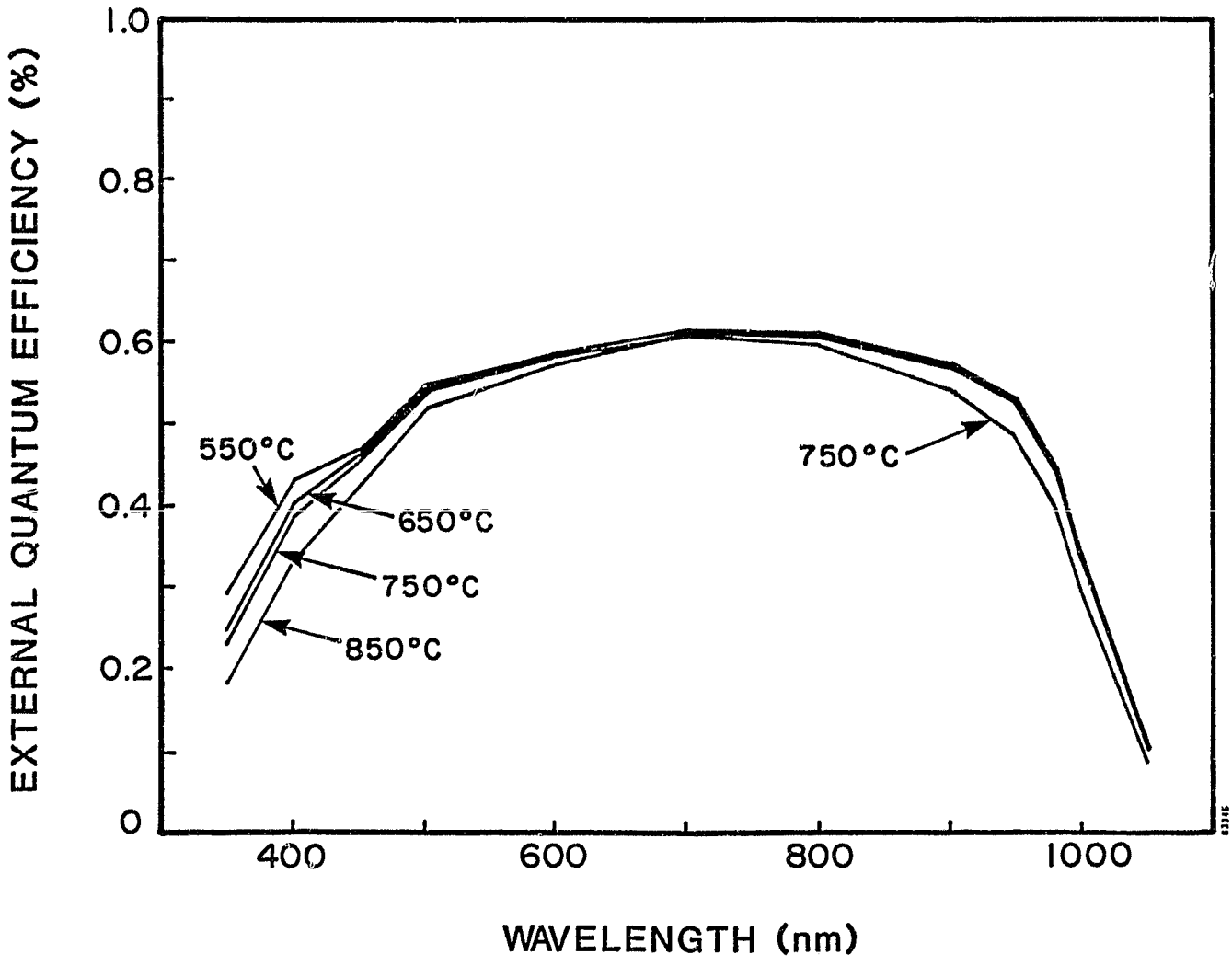

FIGURE 2. EXTERNAL QUANTUM EFFICIENCY OF CZ CONTROL CELLS.

4.2 Silso Solar Cells

Cells were fabricated from Silso and cell performance data are shown in Table 4. Best results were obtained with an activation temperature of 850°C. The results, however, show a curious decrease in efficiency in the temperature range of 650°C to 750°C. Examination of the quantum efficiency (Figure 3) shown a decrease in blue response owning to in-diffusion of the junction, and a decreased red response for the 650°C and 750°C matrix elements. This data may reveal a grain boundary effect; it would be interesting to see if this is an intra-grain or grain boundary effect.

The best Silso cell was fabricated with an activation temperature of 850°C and had the following characteristics: V_{oc} = 533 mV, FF = 5.6%, J_{sc} = 21.9 mA/cm^2 and Eff = 8.8%. With an AR coating, this cell would have an efficiency of nearly 13%.

TABLE 4. AM1 PERFORMANCE OF THE SILSO GROUP.

Activation Temperature	Voc (mV)	Jsc (mA/cm^2)	FF (%)	Eff (%)	Eff x 1.45 (%)
550°C	519 (001)	21.5 (0.3)	73.6 (0.2)	8.20 (0.12)	11.9 (0.2)
650°C	514 (005)	21.0 (0.6)	73.3 (0.5)	7.91 (0.29)	11.5 (0.4)
750°C	519 (003)	21.1 (0.2)	73.8 (0.4)	8.07 (0.12)	11.7 (0.2)
850°C	528 (006)	21.4 (0.4)	75.8 (0.5)	8.56 (0.24)	12.4 (0.3)
3-Step*	523 (005)	20.8 (0.3)	75.0 (1.8)	8.15 (0.25)	11.8 (0.4)

NOTES: Insolation level is 100 mW/cm^2. T = 28°C. Area = 4 cm^2. Standard deviation shown in parenthesis. The 3-step anneal data are reproduced from the baseline experiments.

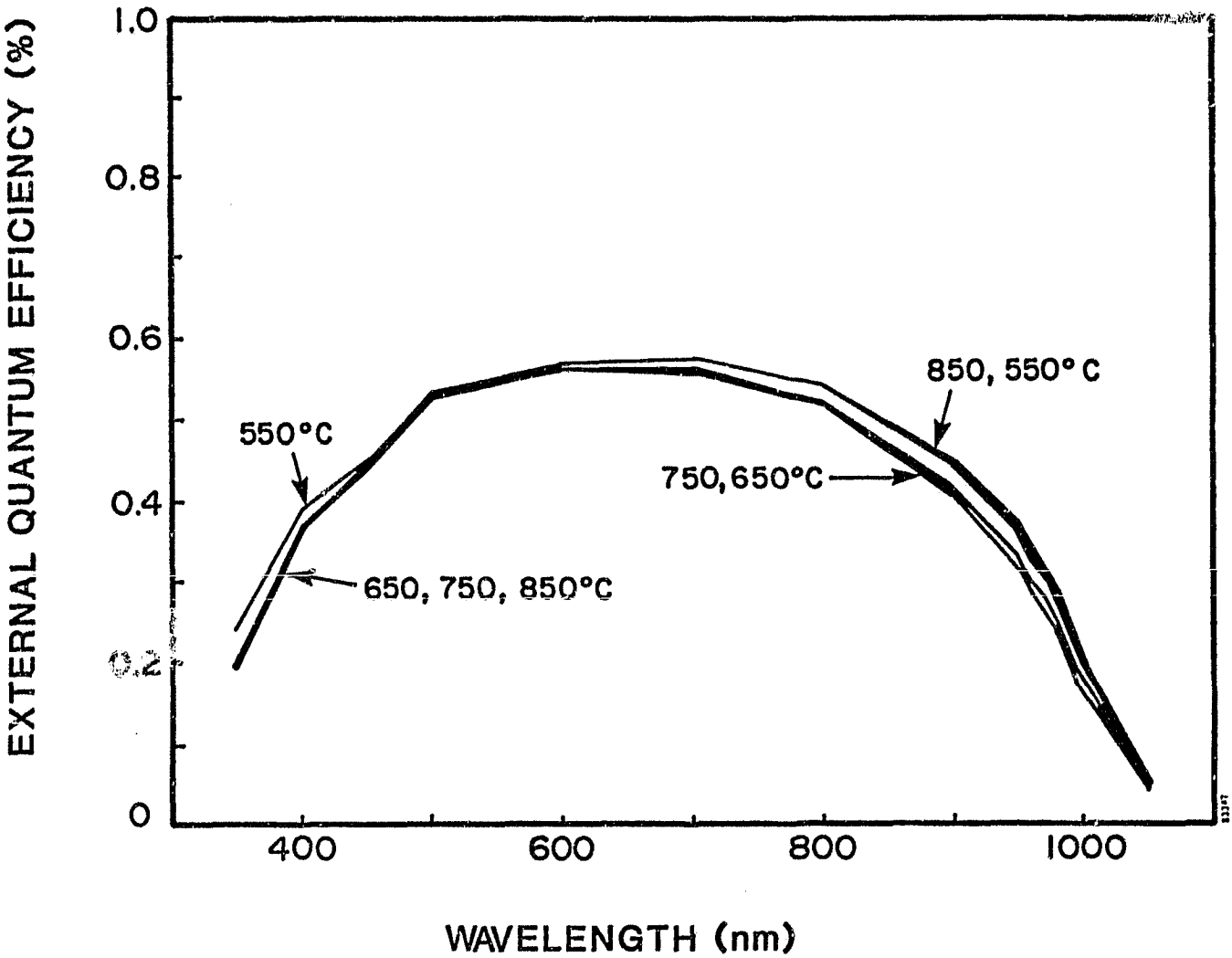

FIGURE 3. EXTERNAL QUANTUM EFFICIENCY OF SILSO CELLS.

4.3 HEM Solar Cells

Cell performance for the HEM cells is shown in Table 5. As with Silso, best results were obtained with an activation temperature of 850°C, and a decrease in performance is found for cells processed at 650°C and 750°C. The external quantum efficiency is shown in Figure 4. The poor performance is most likely the result of degraded diffusion length for anneals at 650°C or 750°C; the mechanism for this effect is unclear.

The best HEM cell was formed with an activation temperature of 850°C. The parameters for this cell were: Voc = 551 mV, FF = 76.5%, Jsc = 21.2 mA/cm^2, and Eff = 8.96%. With a good AR coating, this cell would have an efficiency of about 13%.

TABLE 5. AM1 PERFORMANCE OF THE HEM GROUP.

Activation Temperature	Voc (mV)	Jsc (mA/cm^2)	FF (%)	Eff (%)	Eff x 1.45 (%)
550°C	529 (005)	20.5 (0.6)	74.3 (1.4)	8.07 (0.41)	11.9 (0.6)
650°C	520 (004)	18.9 (0.5)	73.9 (0.7)	7.25 (0.26)	10.5 (0.4)
750°C	526 (007)	19.2 (0.9)	73.5 (1.0)	7.42 (0.43)	10.8 (0.6)
850°C	549 (004)	21.2 (0.1)	76.2 (0.4)	8.86 (0.13)	12.8 (0.2)
3-Step*	553 (010)	20.3 (0.9)	74.0 (2.0)	8.33 (0.53)	12.1 (0.8)

NOTES: Insolation level is 100 mW/cm^2. T = 28°C. Area = 4 cm^2. Standard deviation shown in parenthesis. The 3-step anneal data are reproduced from the baseline experiments.

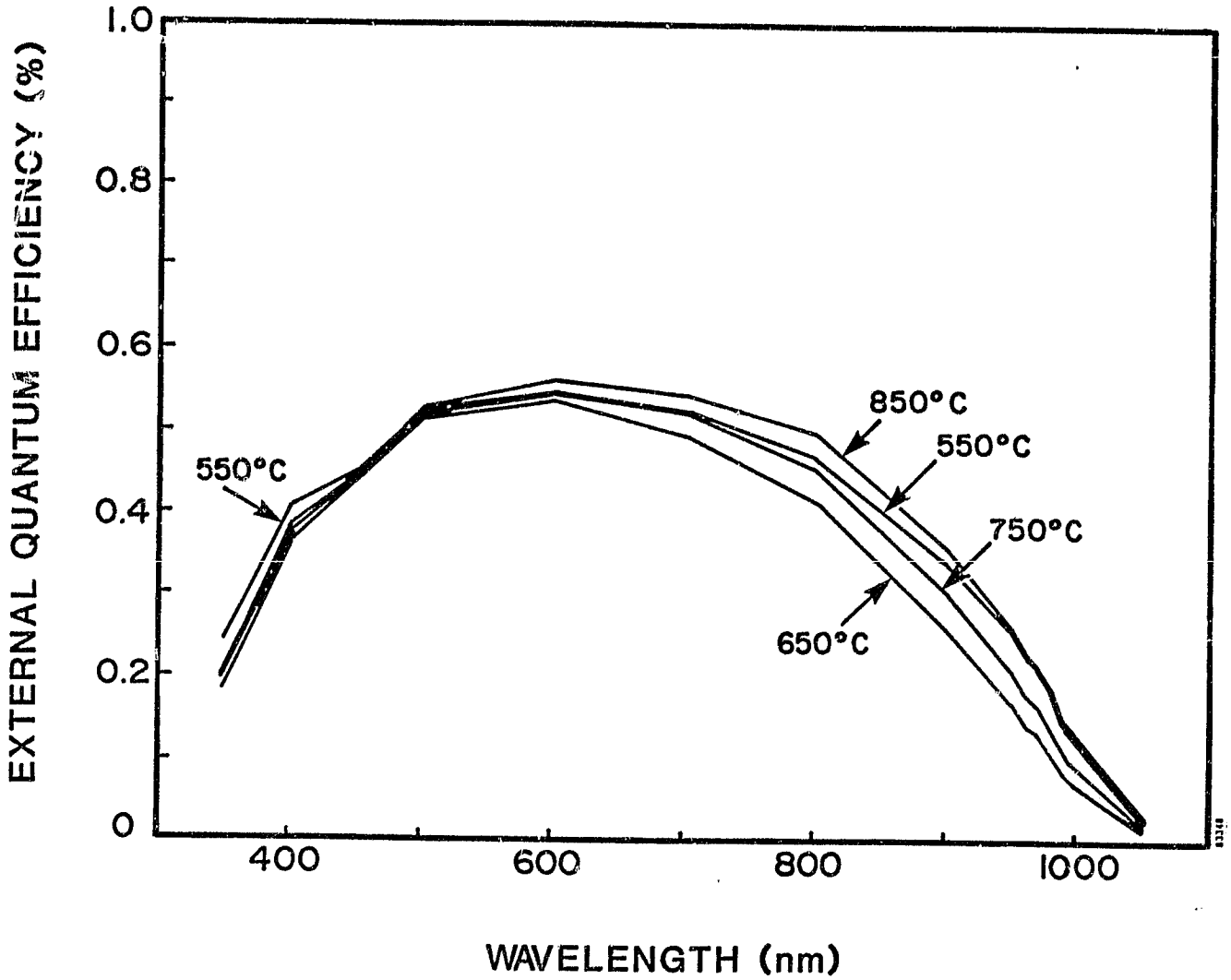

FIGURE 4. EXTERNAL QUANTUM EFFICIENCY OF HEM CELLS.

4.4 EFG Solar Cells

Data for the EFG ribbon cells are shown in Table 6. We have not included the baseline data since baseline cells were fabricated from old EFG silicon. (With the new material, cells of about 11% were fabricated whereas the baseline cells had efficiency of about 8%.)

The EFG material behaves differently than the cast silicon materials. Whereas the cast materials showed decreased performance when annealed at 650°C or 750°C, efficiency of EFG ribbon cells improves with increasing activation temperature. Figure 5, the external quantum efficiency, shows that the higher temperature provides enhanced red response. The red response may be affected by a bulk annealing mechanism or perhaps by gettering of impurities to the junction.

The best EFG solar cell was fabricated with an 850°C activation step. The performance parameters were: Voc = 516 mV, Jsc = 22.31 mA/cm^2, FF = 72.9% and Eff = 8.38. With an AR coating, this cell would have efficiency of about 12%.

After implantation and annealing, the EFG cells had unusually high front sheet resistance, indicating unsatisfactory junction formation. This explains the low FF and perhaps the low Voc. High sheet resistance is most likely the result of ion implantation dose error.

TABLE 6. AM1 PERFORMANCE OF EFG GROUP.

Activation Temperature	Voc (mV)	Jsc (mA/cm^2)	FF (%)	Eff (%)	Eff x 1.45 (%)
550°C	502 (005)	20.2 (0.5)	70.8 (2.5)	7.18 (0.43)	10.4 (0.6)
650°C	512 (002)	21.1 (0.3)	68.1 (1.5)	7.33 (0.16)	10.6 (0.2)
750°C	517 (006)	21.4 (0.2)	70.5 (3.3)	7.81 (0.46)	11.3 (0.7)
850°C	505 (009)	22.1 (0.3)	68.9 (3.6)	7.68 (0.62)	11.1 (0.9)

NOTES: Insolation level is 100 mW/cm^2. T = 28°C. Area = 4 cm^2. Standard deviation shown in parenthesis.

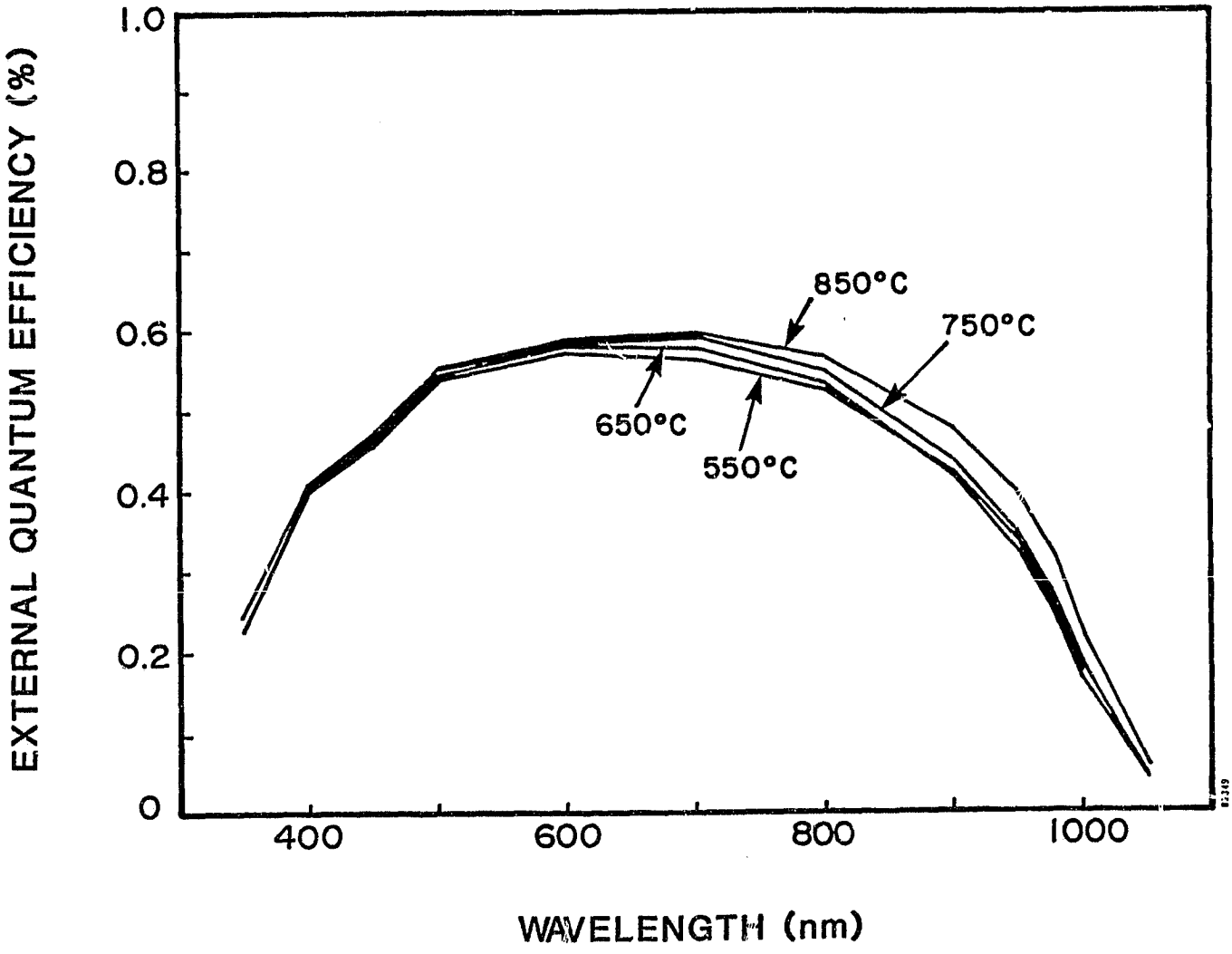

FIGURE 5. EXTERNAL QUANTUM EFFICIENCY OF EFG CELLS.

4.5 Discussion

The data presented allows us to draw some interesting comparisons between the effects of thermal processing on various materials. The CZ control group performs as we expect, indicating that the cell processing has been carried out correctly. There is an indication from the quantum efficiency data that the 750°C anneal may have been contaminated; however, the drop in red response may simply be the result of a slightly inferior starting wafer. In any case, the drop is a small one and does not seem to be evident in the quantum efficiency data for the other materials.

Both HEM and SILSO show some sensitivity to temperatures of 650°C and 750°C. This may be a grain boundary effect; EBIC measurements might be able to determine if this is the case. The EFG improves with increasing temperature. The mechanism operating here is unclear.

Samples of the various wafers will be delivered to the JPL. These non-metallized samples were formed from the same starting blanks as solar cells reported above, and can be used for further analysis. Table 7 lists the sample, material and temperature of the activation anneal.

5.0 CONCLUSIONS

The experiments reported reveal interesting effects of thermal processing on cells formed from poly-Si sheet material. In the final third of the program, we will complete Task 2 by adding (1) SEMIX to the matrix, (2) studying isochronal anneals, and (3) comparing in the results to pulse electron beam annealed solar cells.

TABLE 7. MATERIALS DELIVERED TO JPL

Sample No.	Material	Ta (°C)
1C	C2	850
2C		850
3C		750
4C		650
6C		550
8B	EFG	850
10B		750
11B		650
12B		650
13B		550
14B		550
16B	HEM	850
18B		750
20B		650
21B		550
23B	SILSO	850
24B		850
25B		750
26B		750
27B		650
28B		650
30B		550